



## INELASTIC RESPONSE OF A CONCRETE FRAME BUILDING WITH HIGH-STRENGTH STEEL REINFORCEMENT

F. Carrasco<sup>(1)</sup>, J. A. Pincheira<sup>(2)</sup>

<sup>(1)</sup> Ph.D. Student, Department of Civil and Environmental Engineering, Univ. of Wisconsin-Madison, fcarrasco@wisc.edu

<sup>(2)</sup> Associate Professor, Department of Civil and Environmental Engineering, Univ. of Wisconsin-Madison, jose.pincheira@wisc.edu

### **Abstract**

In recent years, the use of high-strength steel reinforcement in reinforced concrete members has gained significant momentum in the United States. Its use may allow the design of smaller cross sections, or reduce the amount of reinforcement in members which otherwise can be heavily congested. Rebar congestion is a common problem in reinforced concrete columns, beams, and boundary elements of structural walls constructed in high seismic regions, and thus the use of high-strength steel reinforcement emerges as an effective alternative solution to the problem. This trend is also reflected in the recently published provisions of the American Concrete Institute that allow the use of high strength steel reinforcement in seismic areas in some cases.

In this paper, results from numerical simulations of a frame building subjected to earthquake ground motions are presented. The building was designed with either Gr 60 (420 MPa) or with Gr 100 (690 MPa) steel reinforcement but with the same nominal strengths. Modeling of the structural elements were done using fiber-based, distributed plasticity elements using the software SeismoStruct [15]. To validate and assess the robustness of the models, the calculated member response was compared against the results obtained from tests on column specimens published elsewhere in the literature. Both nonlinear static (pushover) and inelastic time-history analyses were conducted.

The response of the buildings is evaluated in terms of base shears, maximum roof drifts and maximum interstory drifts. The data show that the building with Grade 100 steel reinforcement was more flexible after cracking, and consistently developed larger roof and interstory drifts under the ground motions considered. These results suggest that greater structural and nonstructural damage could occur for a building designed with Grade 100 steel (especially at higher performance levels such as immediate occupancy or operational levels).

*Keywords: deformation capacity, fiber-based models, high-strength steel, reinforced concrete, seismic response*



## 1. Introduction

In recent years, the use of steel reinforcement with a yield strength higher than 60 ksi, hereafter referred to as High Strength Steel Reinforcement (HSSR), has gradually increased in popularity within the structural design practice in the United States, mainly due to the potential for cost savings, reduced construction time and reduction of bar congestions [13]. Bar congestion can be especially problematic in seismic zones, where heavily reinforced members may be required in wall boundary elements, beams, and columns.

Although steel with yield strength as high as 100 ksi has been used in Japan and in other countries, its use in the U.S. has been limited. The most recent edition of the ACI Code (ACI 318-19) [1] now allows the use of Grade 100 reinforcement in special structural walls, but limits the yield strength of the longitudinal reinforced steel to 80 ksi in special moment resisting frames. While experimental test data of isolated elements (beams, columns, and walls) reinforced with high-strength steel and subjected to cyclic load reversals exist (Huq et al. [8], Weber-Kamin et al. [17] among others), analyses of buildings structures reinforced with HSSR, subjected to earthquake ground motions are scarce (Rautenberg [14], NIST [13], To D.V. et al. [16]).

## 2. Objective and Scope

The main objective of this study is to compare the seismic response of two 10-story frames designed with Grade 60 and Grade 100 steel reinforcement. The frames were designed for a high seismic zone in California, U.S. The building was originally designed with Grade 60 reinforcement and then with Grade 100 steel so as to achieve the same lateral strength.

Two types of analyses were made: Nonlinear static (Pushover) and inelastic time-history analyses. The nonlinear static analyses were conducted using a parabolic force distribution of the provisions contained in ASCE/SEI 41-17 [2]. In the time-history analyses, the building was subjected to nine strong-motion records obtained from the database available (COSMOS Database [6], CESMD Database [5]) and included vertical and horizontal components of the ground motions. The records were selected to represent a broad range of intensities, duration, and frequency content. The response of the structure is evaluated in terms of the base shears, maximum displacements, and drift profiles.

## 3. Structural Models

### 3.1 Prototype Building (Grade 60 steel reinforcement)

The structure chosen for study consisted of a prototype 10-story reinforced concrete frame building designated for office space, located in the San Francisco Bay Area in California, USA. The floor system consisted of a 5 in. reinforced concrete slab with 12 in. by 22 in. beams in the transverse direction, and 48 in. by 22 in. girders in the longitudinal direction supported on 28 in. by 28 in. interior columns. The perimeter of the building consisted of a moment-resisting frame with 30 in. by 40 in. beams and 40 in. by 40 in. columns. The concrete strength  $f'_c$  was specified as 5000 psi for the slab, and the interior beams and girders, and 6000 psi for the perimeter frame members (beams and columns). The reinforcing steel was specified as Grade 60 for both the longitudinal and transverse reinforcement. A plan view and an elevation of the building are shown in Fig. 1.

Following common practice, interior frames were designed as a gravity load-resisting system, while perimeter frames were designated as special moment-resisting frames. The building was designed using the ASCE/SEI 7-10 [2] standard for computing earthquake-induced loads, and the ACI Code provisions [1] for proportioning and detailing frame members. Based on the location of the building and the site soil properties, the design spectral acceleration at short period,  $S_{DS}$ , and at 1 second period,  $S_{D1}$ , were computed as 1.73g and 1.08g, respectively. Design forces were computed based on an elastic modal analysis of a three-dimensional model of the entire building using cracked section properties per ACI 6.6.3.1 [1].

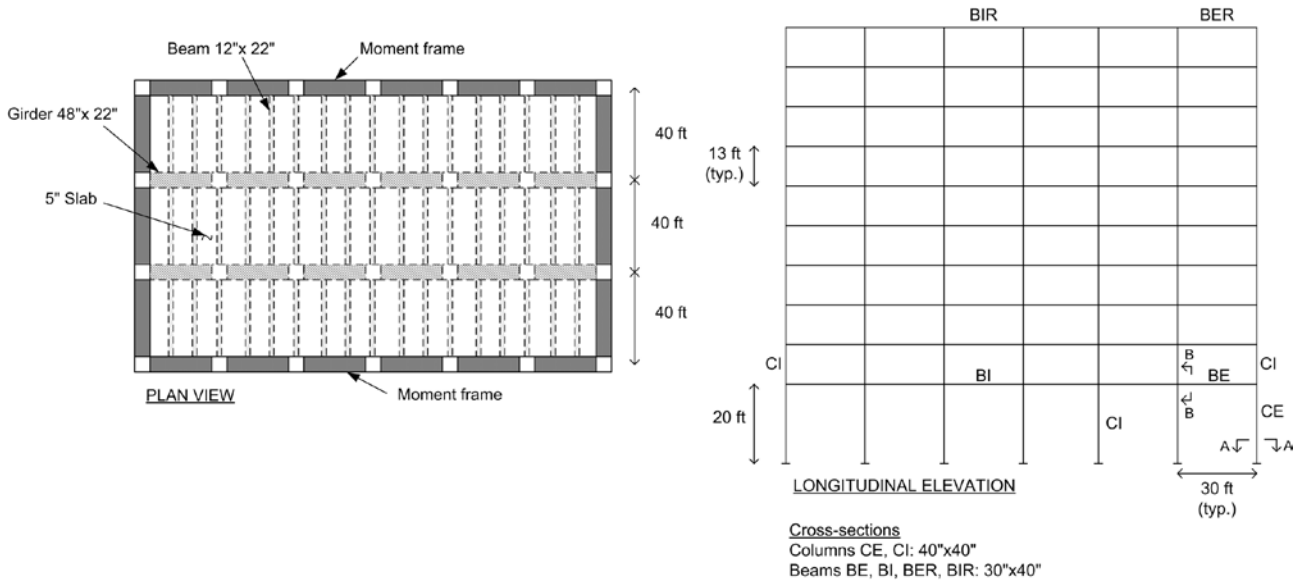


Fig. 1 – Plan view and elevation

Typical Grade 60 reinforcement details of perimeter frame column and beam (cross-sections in Fig. 2). Transverse reinforcement in beams and columns was designed based on the maximum probable flexural strength at the face of the joints, including the effects of the loads acting along the span in beams. Columns were provided with the minimum required flexural strength to reduce the likelihood of a weak-column – strong-beam failure mechanism forming during a strong earthquake. It must be noted that while smaller cross-sections would satisfy strength requirements, final proportioning of the members was governed by stiffness requirements in order to satisfy the maximum interstory drift limits of ASCE/SE 7-10 [2].

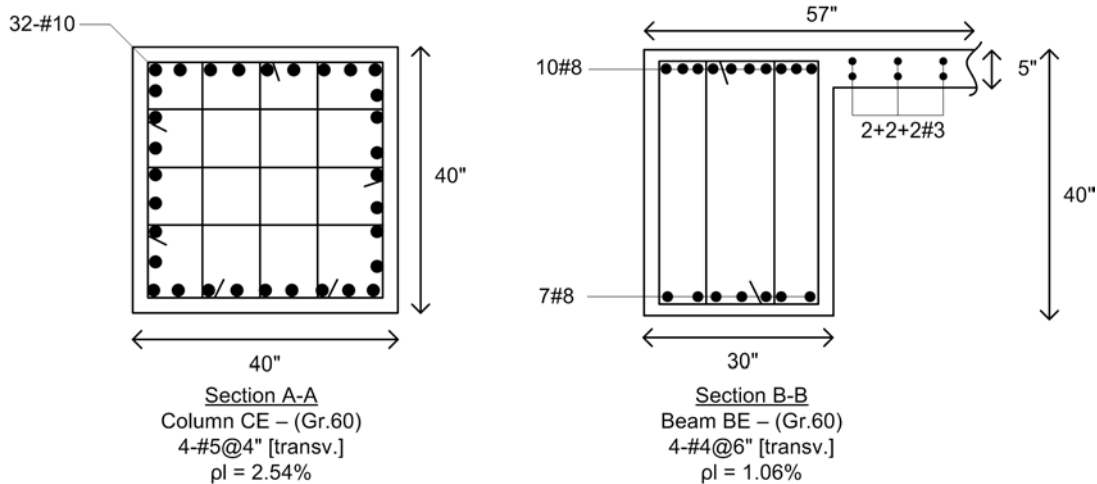


Fig. 2 – Typical details of perimeter frame column and beam cross-sections reinforced with Grade 60 steel (see Fig. 1 for location of cross-sections along the member).

### 3.2 Prototype Building (Grade 100 reinforcement)

For this study, the prototype building was redesigned using Grade 100 steel. Because member size in the building reinforced with Grade 60 steel was governed by stiffness rather than strength requirements, a reduction of the cross-section dimensions of members was not considered. Instead, member size was kept the



same and only the amount of steel reinforcement was modified to obtain approximately the same strength. This was done by specifying a smaller bar size or a smaller number of bars of Grade 100 steel so as to obtain approximately the same nominal flexural strength of beams and columns. Typical reinforcement details of column and beam cross-sections shown earlier in Fig. 2, but with a reduced amount of Grade 100 reinforcing steel are shown in Fig. 3. It is noted that only the longitudinal reinforcement was changed; the amount of transverse reinforcement amount was kept the same.

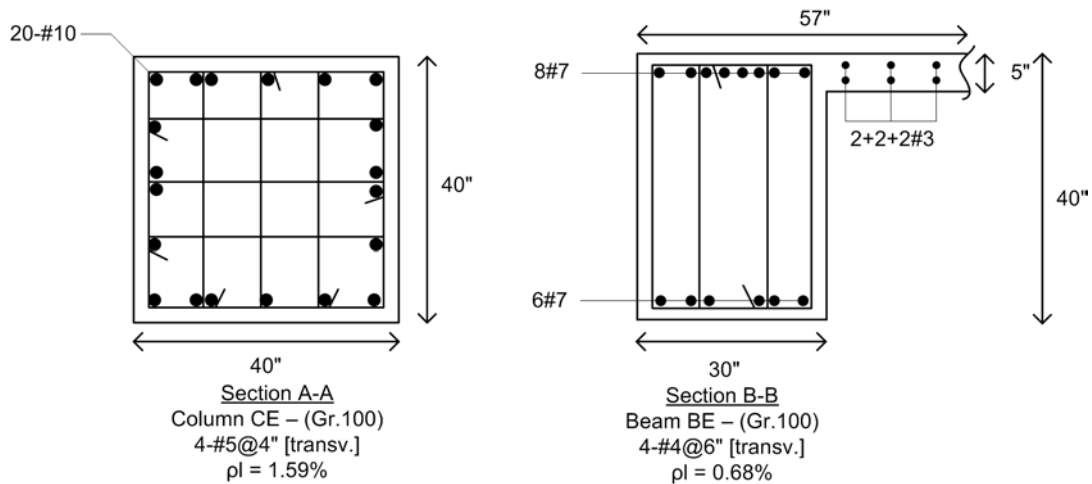


Fig. 3 – Typical details of perimeter frame column and beam cross-sections reinforced with Grade 100 steel (see Fig. 1 for location of cross-sections along the member).

Design interaction diagrams representative of exterior columns and beams reinforced with Grade 60 or Grade 100 reinforcement are shown in Fig. 4. Because of variations in the distribution and arrangement of the steel reinforcement, it is not possible to obtain exactly the same design strength at all levels of axial load. In general, the amount and distribution of the longitudinal reinforcement was chosen so that the design strength was approximately the same at axial loads near the balanced reinforcement ratio. For beams, the reinforcement amount was chosen so that the same design strength was developed at axial loads below  $0.1A_g f'_c$ . In some members, however, such as in columns and beams in the upper stories of the building, the amount of reinforcement was governed by minimum reinforcement requirements for Grade 100 steel.

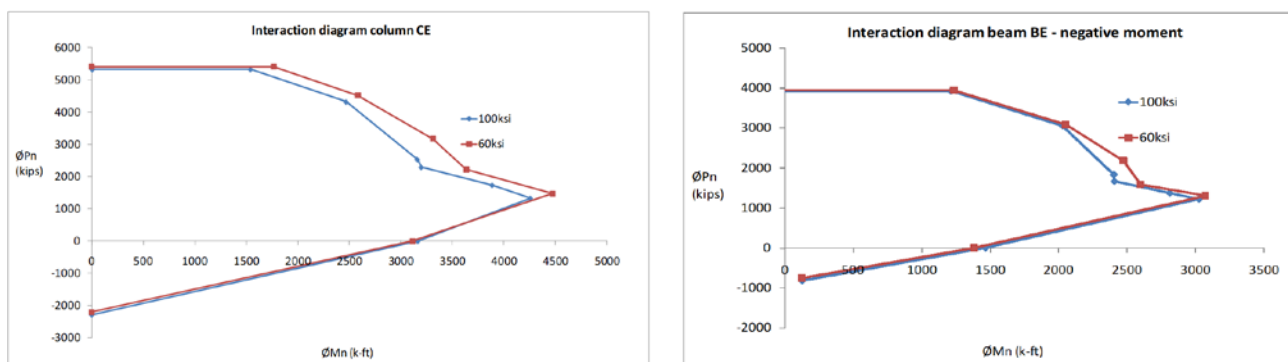


Fig. 4 – Interaction diagram for column CE and beam BE – negative moment

### 3.3 Computational Model

In this section, the main modeling assumptions for conducting inelastic pushover and time-history analyses of the building are described. For simplicity and to reduce the computational effort, the building was idealized in two dimensions and included only the perimeter frames in the longitudinal direction, i.e., the interior frames



were not included in the inelastic analyses. The building mass was lumped in each floor and was proportionally assigned to the perimeter frames so as to match the fundamental period used in the design of the building. All inelastic behavior was assumed to occur in beams and columns, i.e., beam-column joints were assumed to be rigid and infinitely strong. Amplification of deflections and moments due to second order effects (P- $\Delta$  effects) were included in the analyses.

Inelastic analyses of the building were conducted using the finite element based software SeismoStruct [15]. Columns and beams were modeled using force-based, beam-column elements of distributed plasticity. Each member (column or beam) was modeled using 7 integration points along the length (see Fig. 5), where different reinforcement details can be specified for the cross section at each integration point as needed, for example, along the beam span. As shown in Figs. 2 and 3, a portion of the slab was assumed to contribute to the flexural stiffness and strength of the beam for positive (slab in compression), and negative (slab reinforcement in tension) moments.

Each cross section was modeled using 400 fibers. Constitutive relations for the concrete followed the stress-strain relationship proposed by Mander et al. [10] for both unconfined and confined concrete. Steel reinforcement followed the stress-strain relation of Giuffre-Menegotto-Pinto [7]. Examples of the constitutive relationships including the loading, unloading, and reloading rules for the concrete and steel reinforcement are shown in Fig. 6.

Flexure-shear interaction was not included in the models, as the effect of this interaction was considered to be small for these members. Additional deformations due to yield penetration at the ends of the member were not included. While the latter can increase the magnitude of the lateral drifts, they are not expected to significantly affect the comparisons of the building response.

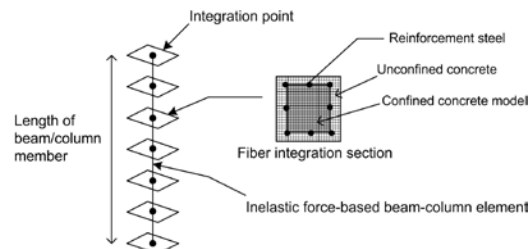


Fig. 5 – Inelastic force-based beam-column element

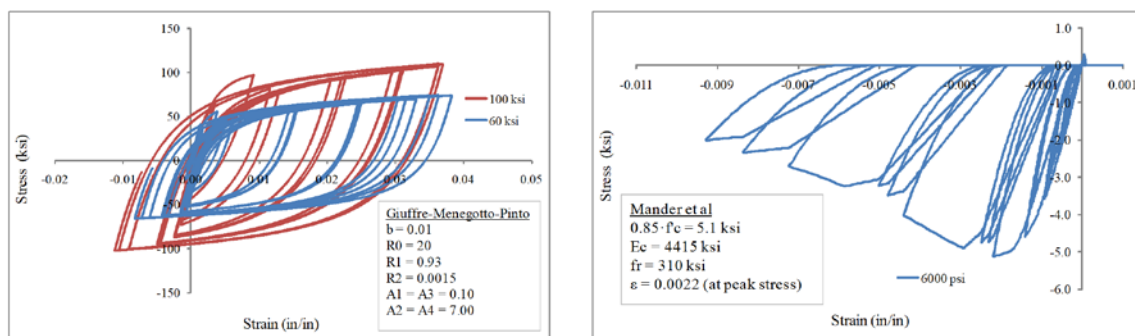


Fig. 6 – Example of stress-strain relationships for the models used in the reinforcement steel and concrete

### 3.4 Validation of Modeling Assumptions

The response obtained with distributed plasticity models have been shown to be sensitive to the choice of the number of integration points [11] and, as for all inelastic models, to the selection of appropriate response parameters. The parameter values used for the behavior of the concrete and steel reinforcement were initially



based on those recommended in the literature and later calibrated using experimental data as described next. The number of integration points was chosen by trial and error by comparing the calculated and experimentally measured response of four columns. As an example, Fig. 7 shows a comparison of the calculated and measured lateral load and lateral drift for a column tested by Lynn [9] and another tested by Rautenberg [14]. For the column tested by Lynn [9], the calculated and measured responses are in very good agreement up to drifts of about 2%. At larger drifts, the tested column showed a sudden loss of strength due to buckling of the longitudinal reinforcement, a behavior that is not included in the present model. In the response of the column tested by Rautenberg [14], the calculated response is not in as good an agreement as for the other column. The model underestimates the measured lateral resistance at up to drifts of about 2% and then it tends to overestimate its resistance. Despite these discordances, the overall response is captured approximately well. At larger drifts (4%), the tested column showed a reduction in the lateral-load carrying capacity first due to shear cracks that damaged the core of the column and finally by buckling of the longitudinal bars. The latter were not included in the models, and thus the model is not able to capture this type of behavior at such large drifts.

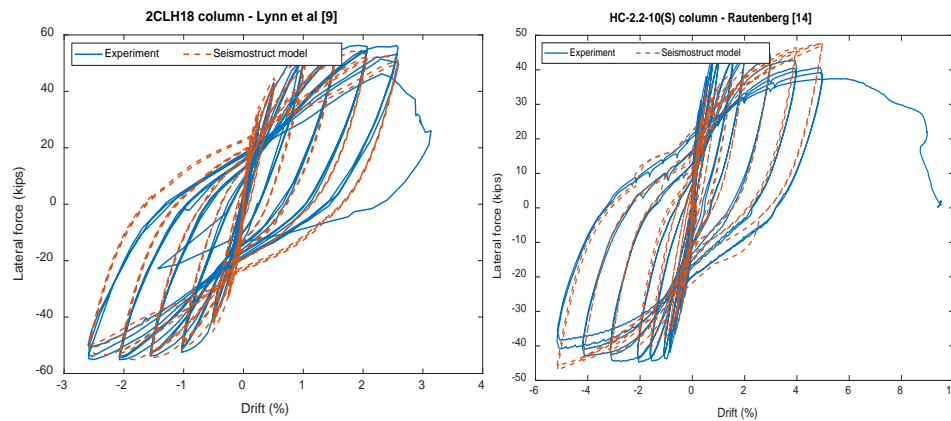


Fig. 7 – Comparison of the cyclic response of the Lynn [9] and Reutenberg [14] columns modeled with SeismoStruct [15].

### 3.5 Analyses

Pushover and inelastic time-history analyses were carried out in this study. The pushover analyses were made using a pseudo-parabolic lateral force distribution over the building height in proportion to the mass in each floor. Inelastic time-history analyses included ground motions in both the horizontal and vertical direction. Viscous damping was specified as 2% mass and stiffness proportional (Rayleigh) damping. However, the mass and stiffness coefficients were calculated so as to reduce the variability of the damping and to maintain a nearly constant damping ratio of 2% as the structure becomes more flexible during the inelastic excursions, as shown in Fig. 8.

Two strain-hardening parameters were used for the steel reinforcement, therefore two sets of analyses were made, one with 0.01 and other with 0.03 strain hardening ratio in the Giuffre-Menegotto-Pinto model [7]. These values were chosen based on recommendations given in past studies and in order to have an upper and lower bound of the effect of this parameter on the inelastic response.

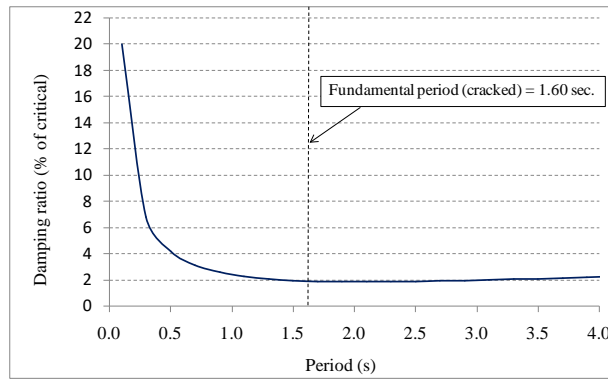


Fig. 8 – Relationship between damping ratio and period of vibration used in this study

### 3.6 Input ground-motions

Nine strong-motion records were selected from the available database (COSMOS [6], CESMD [5]) for the inelastic time-history analyses of the building. Horizontal and vertical ground-motion records were applied simultaneously. The records were chosen to include a broad range of spectral demands within the fundamental period of the building, ground motion duration, and site soil properties. Fig. 9 shows a comparison of the 5% damping acceleration and displacement spectra according to the ASCE/SEI 7-10 [2] used in the design of the building with those computed for the selected records. The characteristics of the records are shown in Table 1.

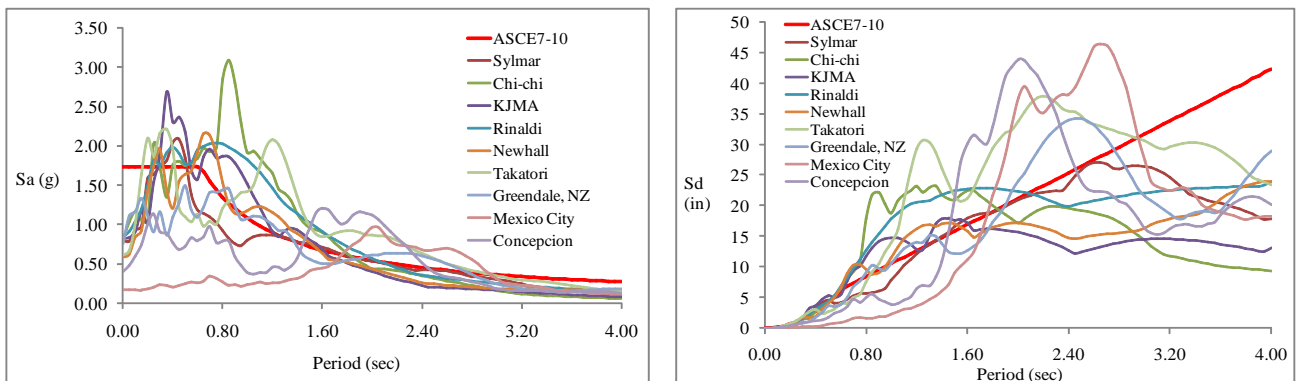


Fig. 9 – Acceleration and displacement spectra of the records selected for study (5% damping)

## 4. Results

### 4.1 Pushover analysis

Base shear coefficient and roof drift relationships for the building reinforced with Grade 60 and with Grade 100 steel are compared in Fig.10. The plots show that even though both, the building reinforced with Grade 60 and Grade 100 steel reinforcement, develop the same lateral strength, the frame with Grade 60 is stiffer at drifts corresponding to first yield. While this result was anticipated because of the reduction in the reinforcement ratio of the members designed with Grade 100, the increase in roof drift at a base coefficient of 0.15, for example, can be significant (about 42%). This result suggests that while the buildings reinforced with either Grade 60 or Grade 100 may have adequate strength to sustain strong earthquakes, the building reinforced with Grade 100 may sustain greater structural and nonstructural damage during low to moderate earthquakes.



Table 1 – Main characteristics of the strong-motion records used in the study

Nº	Earthquake	date	Station	Mw	Depth (km)	PGA (g)
1	Mexico City, Mexico	09-19-1985	SCT B-1 - Comp. N90E SCT B-1 - Comp. Up	8.0	15.0	0.16 0.04
2	Northridge, CA	01-17-1994	Sylmar-6 county Hosp. - Comp. 0 Sylmar-6 county Hosp. - Comp. Up	6.7	18.0	0.80 0.33
3	Northridge, CA	01-17-1994	Rinaldi Station - Comp. S49W Rinaldi Station - Comp. Up	6.7	18.0	0.84 0.85
4	Northridge, CA	01-17-1994	Newhall Fire St. - Comp. 90 Newhall Fire St. - Comp. Up	6.7	18.0	0.58 0.55
5	Kobe, Japan	01-16-1995	KJMA - Comp. 0 KJMA - Comp. Up	6.9	17.9	0.82 0.34
6	Kobe, Japan	01-16-1995	Takatori - Comp. 0 Takatori - Comp. Up	6.9	17.9	0.62 0.27
7	Chi-Chi, Taiwan	09-20-1999	CWB station CHY080 - Comp. 90 CWB station CHY080 - Comp. Up	7.6	6.8	0.81 0.73
8	Canterbury, New Zealand	09-03-2010	Greendale - Comp. N55W Greendale - Comp. Up	7.0	10.0	0.75 0.95
9	Maule, Chile	02-27-2010	Concepcion - Comp. L Concepcion - Comp. Up	8.8	30.1	0.40 0.37

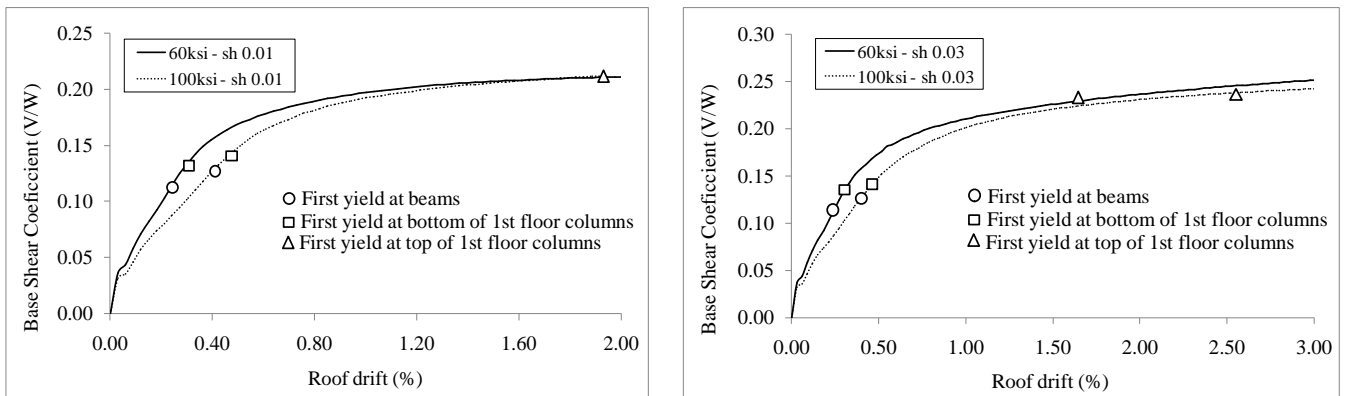


Fig. 10 – Base shear coefficient and roof drift relationships: a) model with strain hardening ratio of 0.01, and b) model with strain hardening ratio of 0.03.

#### 4.2 Time-history analysis

In Fig. 11, the maximum roof drifts obtained with Grade 60 and with Grade 100 reinforcement are compared. The results show that the building reinforced with Gr.100 steel reach larger roof drifts for nearly all of the ground motions, irrespective of the strain hardening ratio considered. The increase in roof drift varied between -0.06% (decrease) and 23.6% (increase) with an average value of 11.2% increase.

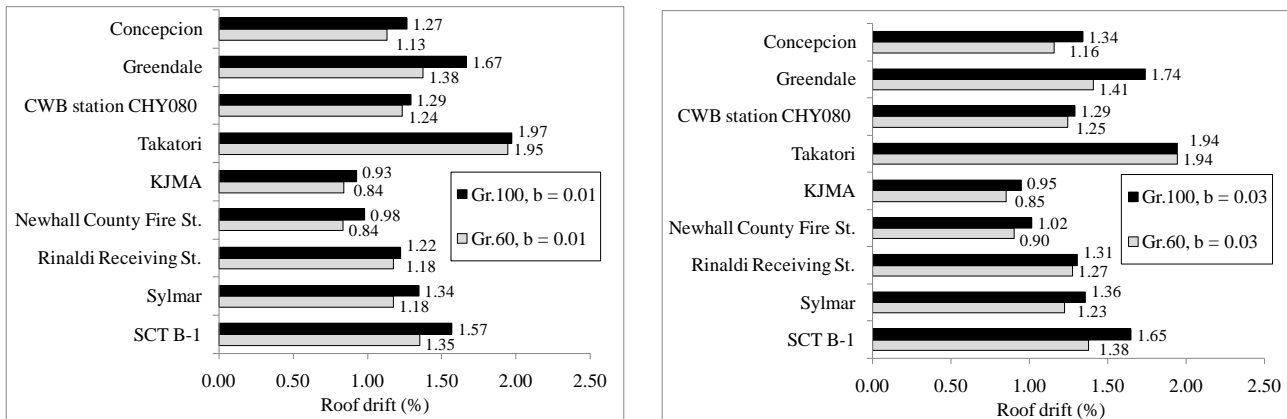


Fig. 11 – Maximum roof drifts (%): a) model with strain hardening ratio of 0.01, and b) model with strain hardening ratio of 0.03

Profiles of the maximum interstory drifts obtained for the nine ground motions considered in this study are shown in Fig. 12. Again, the data show that interstory drifts demands are, with a few exceptions, consistently larger for the building reinforced with Grade 100 in every story.

The data in Figs. 11 and 12 illustrate the difference in the maximum values for the roof and the interstory drifts, respectively, for the buildings reinforces with Grade 60 or Grade 100. However, the largest increase in either roof or interstory drift may not occur during at maximum drift. Fig. 13 shows, for example, the roof drift – time history response for the Mexico City record. It can be seen that the building with Grade 100 reinforcement exhibits much larger drift amplitudes prior to reaching the maximum drift. In fact, they can be twice as large as those of the building with Grade 60 reinforcement. In other words, greater accumulated damage may be expected in those instances, even though the difference in maximum interstory drift at peak displacement may not be as large.

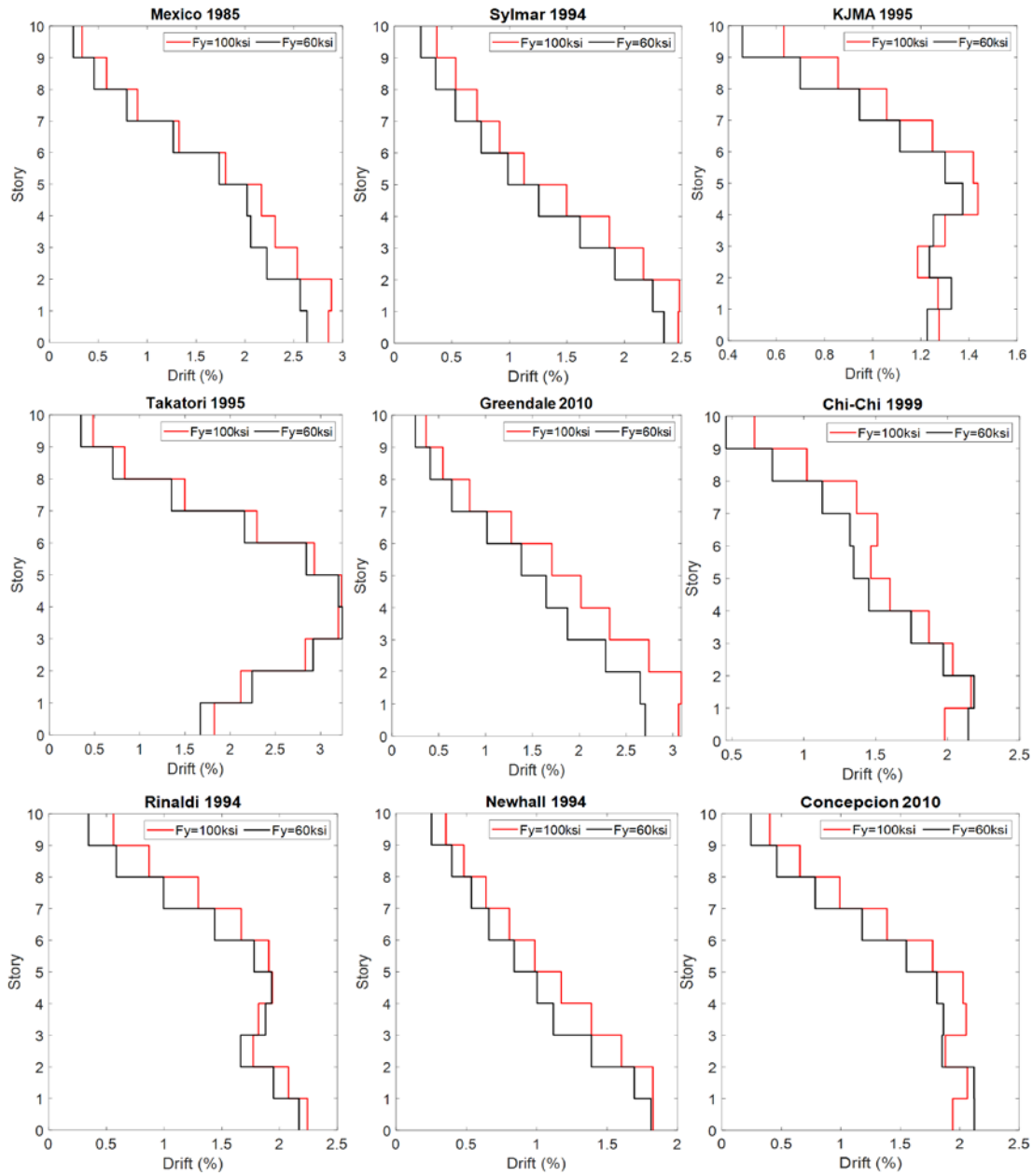


Fig. 12 – Maximum drift profiles for the records used in this study (strain hardening ratio of 0.01)

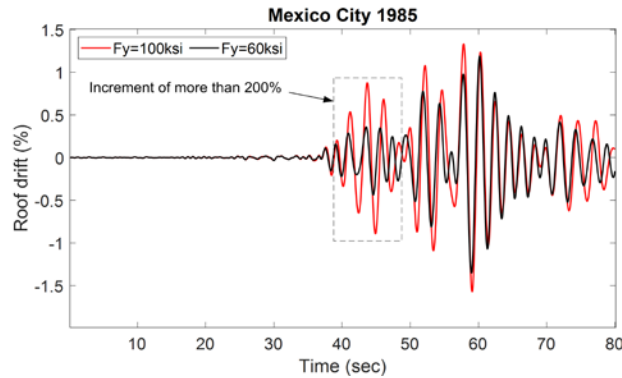


Fig. 13 – Roof – time history – response drifts for the record of Mexico City (hardening ratio of 0.01)



## 5. Summary and Conclusions

In this study, nonlinear static and inelastic time-history analyses of a 10 story frame building reinforced with either Grade 60 or Grade 100 steel reinforcement were conducted. The building was designed for a high seismic region in the U.S. and using the ACI Code provisions for proportioning and detailing its members. Based on the results of this study, the following conclusions can be made.

The results obtained from the nonlinear static (pushover) analyses show that although both buildings were designed for the same lateral strength, the building reinforced with Grade 100 reinforcement can be much more flexible and experience larger drifts after cracking than the structure with Grade 60 reinforcement. For the ground motions considered, inelastic time-history analyses show that the building reinforced with Grade 100 steel consistently developed larger roof and interstory drifts. These results suggest that greater structural and nonstructural damage would be expected for a building designed with Grade 100 steel (especially at higher performance levels such as immediate occupancy or operational levels).

Because the stiffness of the members used in elastic, factored load analyses are based on cross-section dimensions and do not explicitly consider the amount of steel reinforcement, such analyses will not capture the additional flexibility that exhibit members reinforced with HSSR. Additional studies are underway by the authors to suggest changes to the reduction factors from Table 6.6.3.1.1(a) of the ACI code [1] when high-strength reinforcement steel used. Lower moments of inertia are recommended for elastic analyses when high-strength steel is used in design, e.g., the use 80% of the values recommended by the ACI Code [1] seems a reasonable assumption [13].

## 6. Acknowledgement

The first author would like to acknowledge the financial support provided by ANID-CONICYT through their fellowship program “Beca de Doctorado en el Extranjero Becas Chile”. The additional financial support from the Department of Civil and Environmental Engineering and the Neale Silva Scholarship Committee at the University of Wisconsin–Madison is gratefully acknowledged.

## 7. References

- [1] ACI 318 (2014). Building Code Requirements for Structural Concrete (ACI 318-19) and Commentary, American Concrete Institute, Farmington Hills, MI.
- [2] ASCE 7 (2010). Minimum Design Loads for Buildings and Other Structures, American Society of Civil Engineers, Reston, VA.
- [3] ASCE 41 (2017). Seismic Rehabilitation of Existing Buildings, ASCE/SEI Standard 41-17, American Society of Civil Engineers, Reston, VA
- [4] Barin, B. (2002). *Influence of modeling parameters and assumptions on the seismic response of an existing RC building*. A Report to the National Science Foundation, CMS-9624801, Department of Civil and Environmental Engineering, University of Wisconsin–Madison.
- [5] CESMD. (2012). Center for Engineering Strong Motion Data.
- [6] COSMOS. (2011). COSMOS Virtual Data Center.
- [7] Filippou, F. C., Bertero, V. V., & Popov, E. P. (1983). Effects of bond deterioration on hysteretic behavior of reinforced concrete joints.
- [8] Huq, M. S. (2018). *High-Strength Steel Bars in Earthquake-Resistant T-Shaped Concrete Walls*, PhD Dissertation, University of Kansas.



- [9] Lynn, A.C., (2001). “Seismic Evaluation of Existing Reinforced Concrete Building Columns”, *Ph.D. Dissertation*, Department of Civil and Environmental Engineering, University of California, Berkeley.
- [10] Mander, J. B., Priestley, M. J., & Park, R. (1988). Theoretical stress-strain model for confined concrete. *Journal of structural engineering*, 114(8), 1804-1826.
- [11] Mathew, J. (2019). *Analysis of four reinforced concrete columns under cyclic loading using OpenSees*, Advanced Independent Study Report, Department of Civil and Environmental Engineering, University of Wisconsin–Madison.
- [12] McKenna, F., Fenves, G. L., & Filippou, F. C. (2010). OpenSees. *University of California, Berkeley: nd*.
- [13] NIST (2014), “Use of High-Strength Reinforcement in Earthquake-Resistant Concrete Structures”, NIST GCR 14-917-30, National of Standards and Technology, Gaithersburg, MD.
- [14] Rautenberg, J. M., (2011) “Drift Capacity of Concrete Columns Reinforced with High-Strength Steel”. *Ph.D. Dissertation*, School of Civil Engineering, Purdue University.
- [15] Seismosoft, S. (2012). Seismostruct - A computer program for static and dynamic nonlinear analysis of framed structures, available from URL: <http://www.seismosoft.com>.
- [16] To D.V., Sokoli D., Moehle J.P., and Ghannoum W.M. (2018). Seismic Performance of Tall Concrete Special Moment Frames with High-Strength Reinforcement. *Proceedings of the 11th National Conference in Earthquake Engineering*, Earthquake Engineering Research Institute, Los Angeles, CA.
- [17] Weber-Kamin, A. S., Lequesne, R. D., & Lepage, A. (2019). *RC Coupling Beams with High-Strength Steel Bars: Summary of Test Results*. University of Kansas Center for Research, Inc.